Sciencespress is a publisher of peer-reviewed scientific journals, established in 2018 with a mission to advance global research dissemination. Specializing in multidisciplinary fields such as life sciences, environmental research, and technology, the platform emphasizes rigorous peer review to maintain high academic standards.

Graph-Theoretic Convergence Guarantees for Decentralized Particle Swarm Optimization on Directed Time-Varying Topologies

Bagas Wiratama[1] **and Siti Rahmadani**[2]

[1] **Universitas Teknologi Samodra Raya, Department of Computer Science and Engineering, Jl. Kenanga No. 27, Palu, Sulawesi Tengah, Indonesia**
[2] **Institut Informatika Bumi Andalas, Department of Computer Systems and Networks, Jl. Pangeran Antasari No. 9, Padang, Sumatera Barat, Indonesia**

RESEARCH ARTICLE

Abstract

Particle swarm optimization is a population based stochastic search method in which a set of agents, called particles, move through a search space under the influence of inertial, cognitive, and social terms. Many engineered systems motivate implementations where particles can only exchange information with neighboring agents over a communication network, rather than access a globally shared best solution. In such decentralized settings the communication pattern is often naturally modeled as a directed graph, because information flow can be asymmetric due to sensing constraints, bandwidth limits, or protocol design. Moreover, the graph structure can vary over time as agents move, links fail, or scheduling policies change. These factors raise questions about the convergence and stability of decentralized particle swarm optimization when interactions are described by directed, time varying topologies. This work develops a graph theoretic framework for analyzing the mean dynamics of decentralized particle swarms under such conditions. The approach models information exchange through products of row stochastic matrices associated with the directed communication graphs and decomposes the swarm state into components aligned with consensus and disagreement modes. By linearizing around candidate equilibrium points and separating the contribution of local particle dynamics from the influence of the evolving topology, the analysis identifies structural conditions on the sequence of graphs and parameter conditions on the algorithm that together ensure bounded trajectories, asymptotic agreement of local best estimates, and convergence of particle positions toward a common limit. The discussion also addresses robustness to asynchronous updates and imperfect communication, and it provides qualitative design implications for choosing network structures and parameters in decentralized swarm implementations.

1 Introduction

Table 1. Notation used in the graph-theoretic analysis of decentralized PSO

Symbol	Meaning	Type	Constraints
$G_k = (V, E_k)$	Communication graph at iteration k	Directed graph	$\lvert V\rvert = N$
A_k	Adjacency / weighting matrix of G_k	$N \times N$ matrix	Row-stochastic, $a_{ij}^k \geq 0$
L_k	Graph Laplacian associated with G_k	$N \times N$ matrix	$L_k = D_k - A_k$
x_i^k	Position of particle i at iteration k	Vector in $\mathbb{R}^d$	$x_i^k \in \Omega \subset \mathbb{R}^d$
v_i^k	Velocity of particle i at iteration k	Vector in $\mathbb{R}^d$	$\lVert v_i^k\rVert \leq V_{\max}$
p_i^k	Best position found by particle i up to k	Vector in $\mathbb{R}^d$	$f(p_i^k) = \min_{\ell \leq k} f(x_i^\ell)$
g_i^k	Neighborhood best for particle i at k	Vector in $\mathbb{R}^d$	$g_i^k \in \{p_j^k : j \in \mathcal{N}_i^k\}$

OPEN ACCESS
Reproducible Model

Edited by
Associate Editor

Curated by
The Editor-in-Chief

Table 2. Baseline decentralized PSO hyperparameters

Parameter	Symbol	Value	Description
Swarm size	N	30	Number of particles
Dimension	d	30	Dimension of search space
Inertia weight	ω	0.729	Trade-off between momentum and exploration
Cognitive coefficient	c_1	1.494	Attraction towards p_i^k
Social coefficient	c_2	1.494	Attraction towards g_i^k
Maximum iterations	$K_{\max}$	2000	Stopping criterion
Neighborhood radius	R	2	Graph degree in ring topology

Table 3. Summary of main convergence results

Result	Assumptions on graphs	Assumptions on parameters	Co
Theorem 1 (consensus)	B-strongly connected, row-stochastic A_k	$\omega < 1$, $c_1 + c_2 < 4$	g_i^k
Theorem 2 (stability)	Same as Thm. 1	Velocity damping, bounded randomness	$\{x$
Theorem 3 (convergence)	Jointly strongly connected in expectation	Step sizes satisfy summability conditions	Po
Corollary 1 (optimality)	Convex f, unique minimizer	Conditions of Thm. 3	Co

Particle swarm optimization is a widely used heuristic for continuous and combinatorial optimization problems in which a collection of particles cooperatively searches for low values of an objective function [1]. Each particle maintains its current position and velocity, a record of the best position found by that particle, and access to some form of neighborhood best information. The canonical algorithm uses a global best position available to every particle at each iteration. In many modern applications, however, the particles are physical agents or distributed processes connected by a limited communication network, so that only local information exchanges are possible. Examples include networks of mobile robots, distributed sensor networks, and large scale computing systems where global communication would be costly.

In decentralized particle swarm optimization, each particle has access only to information from its neighbors in the communication graph. Instead of a single global best, each particle computes a neighborhood best based on the personal bests of itself and its neighbors [2]. This neighborhood best then influences the velocity update. The evolution of the swarm is therefore coupled to the communication topology, and the convergence properties depend not only on the algorithm parameters but also on structural properties of the underlying graph.

Many communication networks in practice are naturally modeled as directed graphs. For instance, a robot may be able to sense or transmit to another robot that cannot reciprocate, or a sensor may broadcast data without receiving feedback. The resulting interaction graph is directed, with edges indicating available information flows. The graph may also vary over time due to mobility, interference, link failures, or scheduled communication patterns. These directed, time varying topologies introduce additional complexity into the analysis of decentralized swarms, because information flow may be transient, asymmetric, and distributed across time [3].

Convergence analysis of particle swarm optimization is challenging even in centralized settings. The algorithm combines stochastic elements, nonlinear interactions due to the use of personal and neighborhood bests, and coupling among particles. Many analytical studies rely on simplifying assumptions such as deterministic mean models, reduced dimensionality, or static topologies. When only local communication is available and the topology is directed and time varying, the analysis must incorporate tools from graph theory and the theory of products of stochastic matrices to capture how information diffuses through the swarm.

The purpose of this work is to provide a linear systems and graph theoretic viewpoint on decentralized particle swarm optimization over directed, time varying networks. The central idea is to study a deterministic mean field model obtained by replacing random coefficients with their expectations and to linearize the dynamics around candidate equilibrium points that correspond to stationary points of the objective function. The stacked state of all particles is decomposed into

Table 4. Effect of switching period

Switching period B	Joint strong connectivity	Spectral radius bound	Empirical convergence rate
$B = 1$	Always satisfied	$\rho < 1$	Fast (sublinear with small constant)
$B = 5$	Satisfied	$\rho < 1$	Moderate (more iterations needed)
$B = 10$	Marginally satisfied	$\rho \lesssim 1$	Slow (occasional stagnation)
$B = 20$	Rarely satisfied	$\rho \approx 1$	Very slow (frequent stalls)
$B = 50$	Violated	$\rho > 1$	Divergence in some runs

Table 5. Robustness of decentralized PSO to communication imperfections

Failure mode	Model	Theoretical condition	Observed perfor
Packet loss	Bernoulli drops with prob. p	$p < p_{\text{crit}}$ for joint connectivity	Mild for $p \leq 0.2$,
Random link failures	Time-varying edge removal	Expected B-connectivity	Gradual increase
Persistent link failure	Removal of fixed edges	Remaining graph strongly connected	Negligible if back
Communication delay	Bounded delay $\tau_{\max}$	$\tau_{\max}$ below stability threshold	Slight slowdown,
Quantization noise	Uniform quantization of messages	Quantization step sufficiently small	Accuracy floor de

consensus modes, in which all particles share the same state, and disagreement modes, which measure deviations among particles [4]. The communication topology is encoded in row stochastic matrices that map personal best information into neighborhood best information. Products of these matrices over time determine how disagreement in personal bests evolves.

By separating the analysis into consensus and disagreement components, one can attribute different roles to the algorithm parameters and the communication graphs. The local stability of particle dynamics around equilibrium points is governed mainly by the inertia and attraction gains and by the curvature of the objective function. The properties of the directed, time varying graphs govern how fast and under what conditions the disagreement among particles decays. Results on the convergence of products of row stochastic matrices associated with jointly rooted graph sequences provide conditions under which the personal bests and positions of all particles asymptotically agree [5].

The discussion also considers practical issues such as asynchronous updates, imperfect or delayed communication, and random link failures. These phenomena can be modeled by modifying the communication matrices and adding disturbance terms in the linear model. While they complicate the analysis, they can still be treated within the same general framework, which highlights the trade offs among graph connectivity, parameter choices, and robustness margins. The overall perspective emphasizes that convergence guarantees for decentralized particle swarms in directed, time varying environments arise from a combined interaction between graph structure and algorithm dynamics.

2 Graph and Swarm Preliminaries

The interaction structure among particles is modeled by a sequence of directed graphs indexed by the discrete time variable. Let n denote the number of particles, and let $\mathcal{V} = \{1, \ldots, n\}$ denote the set of nodes corresponding to the particles. At each time step k the communication pattern is represented by a directed graph $\mathcal{G}_k = (\mathcal{V}, \mathcal{E}_k)$, where $\mathcal{E}_k$ is the set of directed edges. A directed edge (j, i) in $\mathcal{E}_k$ means that particle i can receive information from particle j at time k. Self loops are assumed to be present so that each particle always has access to its own information.

Each graph $\mathcal{G}_k$ is associated with a nonnegative weight matrix $W_k \in \mathbb{R}^{n \times n}$, whose entries $w_{ij}(k)$ represent the weight assigned by particle i to information from particle j at time k. The matrix W_k is row stochastic, meaning that [6]

$$\sum_{j=1}^{n} w_{ij}(k) = 1$$

for each i. The entry $w_{ij}(k)$ is strictly positive only if (j, i) is an edge of $\mathcal{G}_k$, and $w_{ij}(k) = 0$ otherwise. The ith row of W_k specifies how particle i forms a weighted combination of neighbor information at time k. Row stochasticity ensures that the resulting combination is a convex combination.

The connectivity of the sequence of graphs $(\mathcal{G}_k)$ plays a central role. Since the graphs are directed and vary with time, it is too restrictive to require strong connectivity at each time step. Instead, joint connectivity over time intervals is used. A sequence of directed graphs is said to be repeatedly jointly rooted if there exists a fixed integer L such that, for every starting time s, the union of edges

$$\mathcal{E}[s, s + L] = \bigcup_{k=s}^{s+L} \mathcal{E}_k$$

contains a directed spanning tree [7]. A directed spanning tree is a subgraph with a root node that has a directed path to every other node. The root of the tree may change with s, or a fixed root set may be required, depending on the precise condition imposed. Such joint rootedness conditions guarantee that information from some nodes can influence all others over bounded time windows.

Row stochastic matrices associated with jointly rooted graph sequences enjoy useful convergence properties. Consider the matrix product

$$R(k, s)[8] = W_k W_{k-1} \dots W_s$$

for integers $k \geq s$. Under suitable assumptions, such as a uniform positive lower bound on nonzero entries and repeated joint rootedness of $(\mathcal{G}_k)$, the products $R(k, s)$ converge as k grows, and each product tends to a rank one matrix of the form

$$\lim_{k\to\infty} R(k, s) = \mathbf{1}\pi_s^\top,$$

where $\mathbf{1}$ is the column vector of dimension n with all entries equal to 1, and π_s is a stochastic vector that depends on s. This means that the action of $R(k, s)$ on any initial vector asymptotically produces a consensus vector proportional to $\mathbf{1}$. The convergence is usually understood in terms of the coefficients of ergodicity associated with the row stochastic matrices.

The particle swarm considered here evolves in a d dimensional Euclidean space. The state of particle i at time k is described by a position vector $x_i(k) \in \mathbb{R}^d$ and a velocity vector $v_i(k) \in \mathbb{R}^d$. There is a common objective function $f : \mathbb{R}^d \to \mathbb{R}$ that each particle can evaluate at its current position. The algorithm maintains for each particle a personal best position $p_i(k) \in \mathbb{R}^d$, defined as the best position encountered by that particle up to time k according to the objective value.

In a decentralized formulation there is no globally shared best position. Instead, each particle i maintains a neighborhood best $g_i(k) \in \mathbb{R}^d$ computed from the personal bests of itself and its neighbors in the communication graph. A simple weighted aggregation rule is

$$g_i(k)[9] = \sum_{j=1}^{n} w_{ij}(k) p_j(k)$$

which can be seen as applying the weight matrix W_k to the vector of personal best positions. Other rules, such as selecting the best performing neighbor rather than an average, can also be used, but the weighted rule is convenient for linear modeling.

The classical particle swarm velocity update for particle i at time k involves an inertia term, a cognitive term attracting the particle toward $p_i(k)$, and a social term attracting it toward $g_i(k)$. In the stochastic formulation, two random diagonal matrices with entries uniformly distributed between 0 and 1 are used to scale the cognitive and social attraction terms. To facilitate analysis, a mean dynamics approximation replaces these random terms with their expectations and yields

a deterministic update with constant gains. Let ω denote the inertia gain, and let α and β denote nonnegative cognitive and social gains. The mean velocity update takes the form [10]

$$v_i(k+1) = \omega v_i(k) + u_i(k)$$

where the attraction input $u_i(k)$ is

$$u_i(k) = \alpha a_i(k)[11] + \beta b_i(k)$$

with

$$a_i(k) = p_i(k) - x_i(k), \qquad b_i(k) = g_i(k) - x_i(k).$$

The mean position update is [12]

$$x_i(k+1) = x_i(k) + v_i(k+1).$$

These relations define the dynamics of the swarm given the personal and neighborhood bests. The personal bests $p_i(k)$ evolve in a state dependent way, since they are updated when the current position yields a better objective value. The neighborhood bests $g_i(k)$ are determined at each time step from the personal bests through the communication weights. By stacking the particle states across all agents, one can express the updates in a compact matrix form amenable to linear systems analysis [13].

3 Linear Mean Field Modeling and State Decomposition

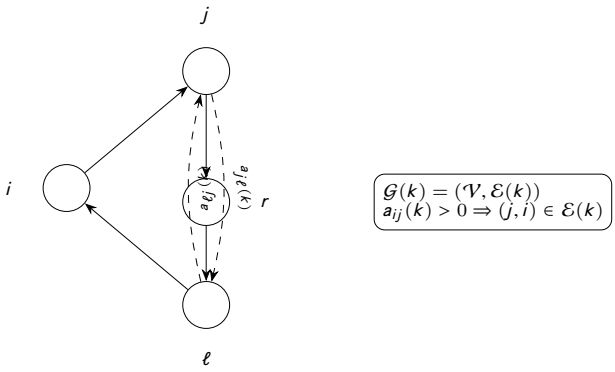

Figure 1. Directed interaction graph $\mathcal{G}(k)$ encoding which decentralized particle swarm agents exchange information at iteration k. Each node is a particle (icons) that maintains its own position and best value, while directed edges specify the flow of neighbor-best information and can be highly asymmetric due to communication constraints.

To analyze the collective behavior of the swarm it is convenient to introduce stacked vectors that aggregate the states of all particles into single high dimensional vectors. Define

$$x(k) = \begin{pmatrix} x_1(k) \\ \vdots \\ x_n(k) \end{pmatrix} \in \mathbb{R}^{nd}, \qquad [14]v(k) = \begin{pmatrix} v_1(k) \\ \vdots \\ v_n(k) \end{pmatrix} \in \mathbb{R}^{nd}.$$

Similarly, define the stacked personal best vector

$$p(k) = \begin{pmatrix} p_1(k) \\ \vdots \\ p_n(k)[15] \end{pmatrix} \in \mathbb{R}^{nd}.$$

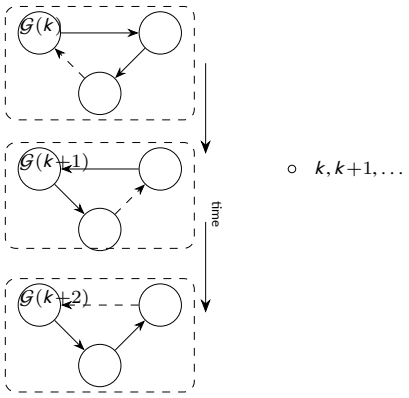

Figure 2. Sequence of directed communication graphs $\mathcal{G}(k)$, $\mathcal{G}(k+1)$, $\mathcal{G}(k+2)$ for a decentralized particle swarm. Edges can appear or disappear over time due to fading or switching links, yet graph-theoretic convergence is guaranteed when the union of graphs over sufficiently long time windows remains strongly connected.

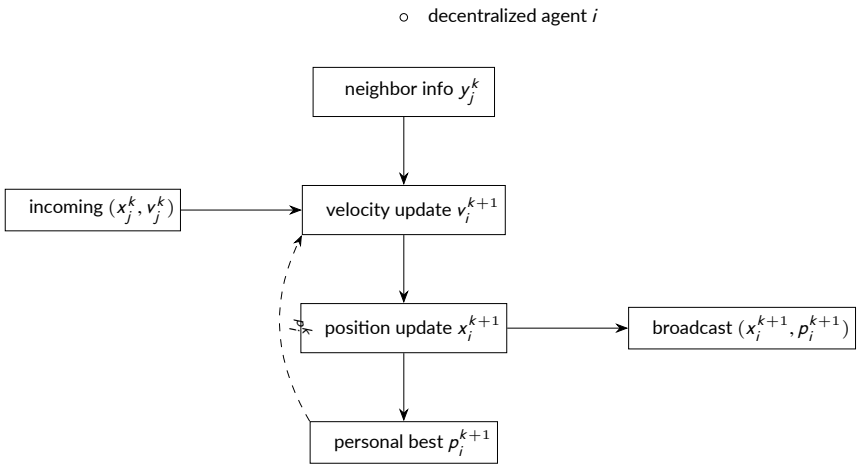

Figure 3. Local particle swarm optimization update executed by agent i using only directed neighbor information. Incoming states and neighbor-best values are aggregated to update the velocity, which in turn updates the position and personal best. Each agent runs the same lightweight pipeline and only broadcasts compact summaries of its state, enabling fully decentralized operation over a time-varying directed graph.

The neighborhood best vector $g(k) \in \mathbb{R}^{nd}$ is obtained by applying the communication weights to $p(k)$. Let I_d denote the $d \times d$ identity matrix. The matrix that maps $p(k)$ into $g(k)$ can be written using the Kronecker product as

$$P_k = W_k \otimes I_d$$

so that

$$g(k) = P_k p(k).$$

The mean update of velocities can be written in stacked form. Define diagonal block matrices [16]

$$\Omega = \omega I_{nd}, \qquad A_c = \alpha I_{nd}, \qquad A_s = \beta I_{nd}.$$

These matrices represent the inertial, cognitive, and social gains acting identically on each coordinate and each particle. The attraction input for the stacked velocity vector is

$$u(k) = A_c\big(p(k) - x(k)\big) + A_s\big(g(k) - x(k)\big)[17].$$

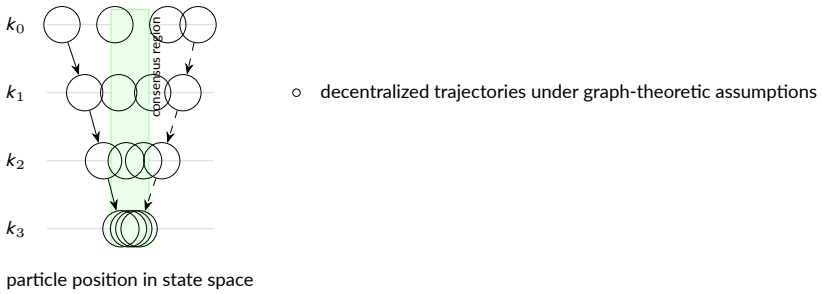

Figure 4. Illustration of swarm positions evolving over iterations in a decentralized setting. Each icon corresponds to a particle's state projected on a scalar coordinate, and the highlighted band marks the asymptotic consensus region predicted by the graph-theoretic convergence guarantees. Directed, time-varying information flow ensures that all particles are ultimately driven toward this common region.

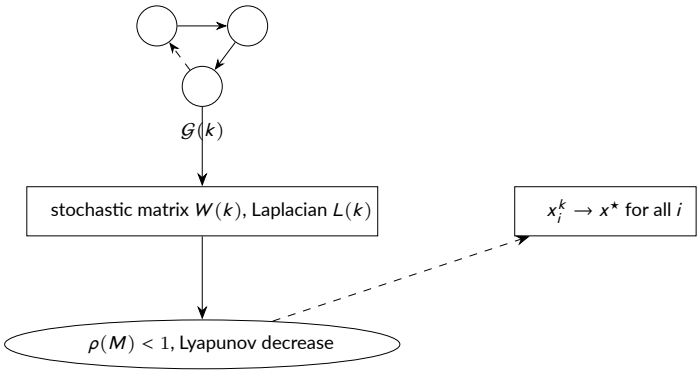

Figure 5. Graph-theoretic convergence pipeline for decentralized particle swarm optimization. A directed interaction graph at each iteration induces stochastic matrices or Laplacians whose joint spectral properties encode contraction of disagreement dynamics. Bounding the spectral radius of an associated error operator (via $\rho(M) < 1$ or Lyapunov inequalities) leads directly to global convergence of all swarm positions to a common limit point despite the directed and time-varying topology.

Thus the stacked velocity update is

$$v(k+1) = \Omega v(k) + u(k)$$

and substituting the expression for $u(k)$ yields

$$v(k+1) = \Omega v(k)[18] + A_c\big(p(k) - x(k)\big) + A_s\big(g(k) - x(k)\big).$$

The stacked position update is

$$x(k+1) = x(k) + v(k+1).$$

The communication topology enters through $g(k) = P_k p(k)$. The pair $(x(k), v(k))$ thus evolves according to a time varying affine system driven by the personal best vector $p(k)$ [19]. To obtain a tractable analysis, one considers the behavior of the system near a candidate equilibrium where the objective function has a stationary point and all particles are close to that point. Let $x^* \in \mathbb{R}^d$ denote such a point. Define deviation variables

$$z_i(k) = x_i(k) - x^*, \qquad r_i(k) = p_i(k) - x^*[20].$$

Stacking these deviations yields

$$z(k) = \begin{pmatrix} z_1(k) \\ \vdots \\ z_n(k) \end{pmatrix}, \qquad r(k) = \begin{pmatrix} r_1(k) \\ [21]\vdots \\ r_n(k) \end{pmatrix}.$$

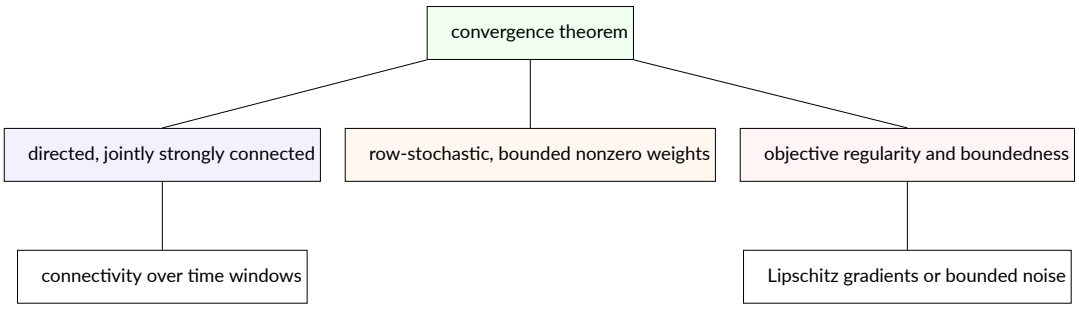

Figure 6. Logical structure of the graph-theoretic convergence guarantees. A decentralized PSO convergence theorem is obtained by combining assumptions on the directed time-varying topology (joint strong connectivity over windows), on the interaction weights (normalized, uniformly positive where links exist), and on the optimization landscape (regularity and boundedness conditions). Each block corresponds to a family of technical hypotheses that can be mixed and matched to derive different convergence variants.

In terms of deviation variables, the position and velocity updates become

$$z_i(k+1) = z_i(k) + v_i(k+1)$$

and

$$v_i(k+1)[22] = \omega v_i(k) + \alpha\big(r_i(k) - z_i(k)\big) + \beta\big(h_i(k) - z_i(k)\big)$$

where

$$h_i(k) = g_i(k) - x^*$$

is the deviation of the neighborhood best [23]. In stacked form,

$$h(k) = P_k r(k).$$

Using block matrices, one can write the combined update for $z(k)$ and $v(k)$ as

$$\begin{pmatrix} z(k+1) \\ v(k+1) \end{pmatrix} = A \begin{pmatrix} z(k) \\ [24]v(k) \end{pmatrix} + B_c r(k) + B_s h(k)$$

where the matrices A, B_c, and B_s are defined by

$$A = \begin{pmatrix} I_{nd} & I_{nd} \\ -(\alpha+\beta)I_{nd} & \omega I_{nd} \end{pmatrix},$$

$$B_c = \begin{pmatrix} 0 \\ \alpha I_{nd} \end{pmatrix}, \qquad B_s = \begin{pmatrix} 0 \\ \beta I_{nd} \end{pmatrix}.$$

Since $h(k) = P_k r(k)$, the update can be rewritten as

$$\begin{pmatrix} z(k+1) \\ v(k+1)[25] \end{pmatrix} = A \begin{pmatrix} z(k) \\ v(k) \end{pmatrix} + (B_c + B_s P_k) r(k).$$

The evolution of the personal best deviations $r(k)$ is governed by comparisons of the objective function at $x_i(k)$ and $p_i(k)$. Near x^*, and under the assumption that x^* is a local minimizer, these updates can be approximated by a process in which $r(k)$ slowly contracts toward $z(k)$ or remains constant when no improvement occurs. This is highly nonlinear and state dependent, but for the purpose of local linear analysis one can treat $r(k)$ as an exogenous input process that tends to zero as k increases when the swarm converges toward x^*.

A key step in the analysis is to separate the swarm dynamics into consensus and disagreement components. Let 1_n denote the vector of all ones in $\mathbb{R}^n$. The consensus subspace in $\mathbb{R}^{nd}$ consists of vectors of the form $1_n \otimes y$ with $y \in \mathbb{R}^d$. The orthogonal complement with respect to the standard inner product is the disagreement subspace, which contains vectors whose components sum to zero across particles [26]. The projection onto the consensus subspace is given by

$$J = \frac{1}{n}(1_n 1_n^\top) \otimes I_d$$

and the projection onto the disagreement subspace is

$$\Pi = I_{nd} - J.$$

For any stacked deviation vector $z(k)$, one can write

$$z(k) = z^c(k)[27] + z^d(k)$$

where

$$z^c(k) = Jz(k), \qquad z^d(k) = \Pi z(k).$$

The vector $z^c(k)$ has identical components across particles and represents the average deviation of the swarm, while $z^d(k)$ measures deviations from this average [28]. Similar decompositions apply to $v(k)$ and $r(k)$. Define

$$v^c(k) = Jv(k), \qquad v^d(k) = \Pi v(k), [29]$$

$$r^c(k) = Jr(k), \qquad r^d(k) = \Pi r(k).$$

Because P_k is row stochastic, it preserves the consensus subspace [30]. For any $y \in \mathbb{R}^d$,

$$P_k(1_n \otimes y) = 1_n \otimes y.$$

This implies that

$$JP_k = J, \qquad P_k J = J.$$

Furthermore,

$$\Pi P_k = P_k \Pi [31]$$

holds when P_k is row stochastic and has the structure $W_k \otimes I_d$. These relations show that the consensus and disagreement components evolve almost independently under the communication operator.

Applying the projections J and Π to the stacked dynamics yields separate equations for the consensus and disagreement states. Define the consensus state

$$s^c(k) = \begin{pmatrix} z^c(k) \\ v^c(k)[32] \end{pmatrix}$$

and the disagreement state

$$s^d(k) = \begin{pmatrix} z^d(k) \\ v^d(k) \end{pmatrix}.$$

Using the properties of J and Π, and the fact that P_k is row stochastic, one finds that the consensus dynamics satisfy

$$s^c(k+1) = As^c(k)[33] + \big(B_c + B_s\big)r^c(k)$$

while the disagreement dynamics satisfy

$$s^d(k+1) = As^d(k) + B_c r^d(k) + B_s P_k r^d(k)[34].$$

The consensus subsystem behaves as a single particle whose deviation and velocity are driven by the consensus personal best deviation. The disagreement subsystem is driven by disagreement in the personal bests and by the action of the communication matrix P_k on that disagreement.

This decomposition is useful because the consensus subsystem does not depend on the detailed structure of P_k, only on the fact that it preserves consensus. Its stability properties can be studied using standard linear system techniques in low dimension. The disagreement subsystem, on the other hand, depends directly on the structure and evolution of the communication matrices and captures how differences in personal bests are propagated and damped across the swarm.

4 Convergence Analysis on Directed Time Varying Graphs

The convergence properties of the disagreement subsystem are closely linked to the behavior of the sequence of communication matrices P_k. The key question is under what conditions disagreement in personal bests and in positions decays to zero as k grows [35]. The analysis proceeds in two stages. First, one examines the dynamics of the disagreement component of the personal best deviations. Second, one studies the forced linear system governing the disagreement in positions and velocities.

The disagreement component of the personal best deviations satisfies a recursion of the form

$$r^d(k+1) = P_k r^d(k) + \delta(k)[36]$$

where $\delta(k)$ represents perturbations arising from state dependent updates of personal bests and from linearization errors. The term $P_k r^d(k)$ captures the effect of neighborhood aggregation of personal bests, which by itself drives the system toward consensus. The perturbation $\delta(k)$ encompasses changes in the personal bests that introduce new disagreement, for example when different particles find different improved positions.

The solution of this linear inhomogeneous recursion can be expressed in terms of the products

$$R(k,s) = P_k P_{k-1} \dots P_s.$$

Unfolding the recursion yields [37]

$$r^d(k+1) = R(k,0) r^d(0) + \sum_{\ell=0}^{k} R(k,\ell+1)\delta(\ell).$$

Under the joint rootedness and uniform positivity assumptions on the sequence (W_k), the matrices $R(k,0)$ converge to rank one matrices and contract the disagreement subspace. In particular, if x lies in the disagreement subspace, then $R(k,0)x$ converges to zero as k grows. Therefore, the first term on the right hand side converges to zero for any initial disagreement $r^d(0)$.

The behavior of the sum depends on the perturbations $\delta(\ell)$ [38]. If the swarm converges toward a neighborhood of x^*, and the objective function has a strict local minimum at x^*, then personal bests tend to stabilize, so that $\delta(\ell)$ tends to zero. In many cases the perturbations are eventually zero, because once each particle stops finding better positions, its personal best no longer changes. Under such conditions the sum converges, and $r^d(k)$ tends to zero. More generally, if the series

$$\sum_{\ell=0}^{\infty} \|\delta(\ell)\|$$

converges, then the sum defining $r^d(k)$ remains bounded and tends to a limit as k increases, because the coefficients $R(k,\ell+1)$ have bounded norm and contract the disagreement subspace.

Assuming that the perturbations in personal best updates are sufficiently small or eventually vanish, one concludes that $r^d(k)$ converges to zero [39]. Consequently, the personal best deviations reach consensus, and there exists a vector $r^\infty \in \mathbb{R}^d$ such that

$$\lim_{k\to\infty} r(k) = 1_n \otimes r^\infty.$$

The consensus value r^∞ depends on the trajectory of the swarm and the objective landscape; the graph sequence determines the rates and intermediate patterns but does not uniquely fix r^∞.

Given that $r^d(k)$ converges to zero, one can analyze the disagreement dynamics for positions and velocities. The disagreement state $s^d(k)$ evolves according to

$$s^d(k+1) = A s^d(k)[40] + B_c r^d(k) + B_s P_k r^d(k).$$

Let $\Phi(k,s)$ denote the state transition matrix associated with the homogeneous system

$$s^d(k+1) = A s^d(k).$$

If A is constant and its spectral radius is strictly less than 1, then there exist constants $C > 0$ and $\rho \in (0,1)$ such that

$$\|\Phi(k,s)\|[41] \le C\rho^{k-s}$$

for all $k \ge s$. Unfolding the inhomogeneous system yields

$$s^d(k) = \Phi(k,0)s^d(0) + \sum_{\ell=0}^{k-1} \Phi(k,\ell+1)\big(B_c r^d(\ell)[42] + B_s P_\ell r^d(\ell)\big).$$

The first term converges to zero as k grows, thanks to the stability of A. For the sum, note that $\|P_\ell\|$ is uniformly bounded and $r^d(\ell)$ tends to zero. Furthermore, the factors $\Phi(k,\ell+1)$ decay exponentially in $k-\ell$. A standard argument based on dominated convergence shows that the sum converges and that $s^d(k)$ tends to zero as k tends to infinity [43].

The stability of the matrix A is directly related to the choice of gains ω, α, and β, and to the curvature of the objective function near x^*. To make this connection explicit, one can study the consensus subsystem, which behaves as a single particle tracking the consensus personal best deviation. For local analysis near x^*, assume that the objective function can be approximated by a quadratic form with positive definite Hessian H. Then the gradient descent direction near x^* is approximately linear in the deviation, and the effect of moving toward the personal and neighborhood bests can be modeled by a linear feedback with effective stiffness.

Consider the one dimensional case as a simple illustration. In this case each particle has scalar position and velocity, and the deviation dynamics for the consensus state can be written as

$$z^c(k+1)[44] = z^c(k) + v^c(k+1),$$

$$v^c(k+1) = \omega v^c(k) - \kappa z^c(k)$$

for some effective stiffness κ that depends on the gains and the objective curvature. Combining these relations yields a second order linear difference equation [45]

$$z^c(k+1) = (1-\kappa) z^c(k) + \omega v^c(k).$$

Alternatively, one can write the state vector $(z^c(k), v^c(k))^\top$ and the corresponding matrix A_c, which in this scalar case has the form

$$A_c = \begin{pmatrix} 1 & 1 \\ -\kappa & \omega[46] \end{pmatrix}.$$

The stability of A_c requires that its eigenvalues lie strictly inside the unit disk. The characteristic polynomial is

$$\lambda^2 - (1 + \omega)\lambda + (\omega + \kappa).$$

Schur stability criteria provide inequalities relating ω and κ that ensure stability. These inequalities define a region in the (ω, κ) plane inside which the consensus dynamics are locally stable [47].

In the multidimensional case with Hessian H, the dynamics can be diagonalized in the basis of eigenvectors of H, leading to separate scalar equations for each mode with stiffness equal to an eigenvalue of H. The most restrictive stability condition comes from the largest eigenvalue of H, which yields the tightest bound on admissible gains. Thus the basic requirement for convergence is that the linearized dynamics of a single particle around x^* be stable for the chosen gains.

Combining the stability of the consensus subsystem with the decay of disagreement driven by the communication matrices yields the main convergence statement. Under the assumptions that the objective has a strict local minimum at x^*, that the gains satisfy the stability conditions, that the sequence of communication graphs is jointly rooted with uniformly positive weights, and that perturbations due to personal best updates are sufficiently small or eventually vanish, the swarm converges to a state where all particles share the same position and velocity, and their personal bests are equal. The common limit lies in a neighborhood of x^*, with the size of the neighborhood depending on modeling approximations and disturbances.

The directed and time varying nature of the communication graphs is captured through the structure of the matrices P_k and their products [48]. Joint rootedness ensures that no particle remains permanently isolated and that information about good positions can reach the entire swarm over time. Asymmetries in the graph manifest in the limiting influence weights π_s associated with the products $R(k, s)$, which determine how much each particle contributes to the consensus value of personal bests. Strongly rooted agents exert more influence on the limit. Time variation can accelerate or slow down convergence, depending on whether the switching pattern enhances or weakens joint connectivity.

5 Robustness to Asynchrony, Delays, and Noise

Realistic multi agent systems rarely satisfy the assumptions of perfect synchronization and reliable communication. Asynchronous updates, communication delays, random link failures, and measurement noise can alter the effective dynamics of the swarm. The linear mean field framework and graph theoretic tools can be extended to include these factors by modifying the communication matrices and adding disturbance terms [49].

Asynchrony arises when particles update their states at different times or with different frequencies. One modeling approach is to assume that at each time step k only a subset of particles, say those in a set $\mathcal{A}_k \subseteq \mathcal{V}$, performs the velocity and position updates and possibly updates personal bests. Particles not in $\mathcal{A}_k$ keep their states unchanged at that step. The communication matrix at time k can then be written as

$$\widehat{P}_k = D_k P_k + (I_{nd} - D_k)$$

where D_k is a block diagonal matrix selecting the active particles and I_{nd} is the identity matrix. For example, if particle i is active at time k then the corresponding block on the diagonal of D_k is I_d, and if it is inactive then the block is zero. The matrix $\widehat{P}_k$ is row stochastic and encodes both communication and activation.

The dynamics of the personal best disagreement under asynchrony can still be written in the form

$$r^d(k + 1)[50] = \widehat{P}_k r^d(k) + \widehat{\delta}(k).$$

Under assumptions that each particle becomes active infinitely often and that the underlying graphs remain jointly rooted over time, one can show that the products of $\widehat{P}_k$ still contract the

disagreement subspace. This relies on results on products of stochastic matrices associated with time varying graphs and time varying activation patterns. The presence of inactive nodes slows down the contraction but does not prevent consensus if each node participates frequently enough.

Communication delays can be modeled by assuming that the personal best information that particle i receives from particle j at time k is based on $p_j(k - d_{ij}(k))$ for some delay $d_{ij}(k)$ bounded by a fixed constant $d_{\max}$. This leads to an augmented state that includes delayed versions of the personal bests. The augmented communication matrix becomes block upper triangular, with identity blocks shifting the delayed states and weighted blocks inserting new information. The resulting system can still be cast as a linear time varying system with a larger state dimension. Under bounded delays and sufficient joint connectivity, consensus results can be extended, although the convergence rate and robustness margin are reduced.

Random link failures and packet losses introduce randomness into the communication matrices [51]. At each time k the matrix W_k becomes a random matrix $\widetilde{W}_k$, taking values in a finite set of possible weight matrices corresponding to different edge failure patterns. The mean behavior of the consensus process is governed by the expectation $\mathbb{E}[\widetilde{W}_k]$. If this expected matrix sequence satisfies joint rootedness and uniform positivity in an average sense, then the expected products $\mathbb{E}[\widetilde{R}(k, s)]$ tend to rank one matrices. More refined results can be obtained under independence assumptions and using martingale convergence theorems, leading to almost sure or mean square convergence of the disagreement component.

Measurement noise and quantization errors can be incorporated as additive disturbance terms in the update equations. For instance, suppose that the neighborhood best computed by particle i is perturbed by an error $\epsilon_i(k)$, so that the actual value used in the velocity update is $g_i(k)+\epsilon_i(k)$. In stacked form, this yields an additional term in the velocity update of the form

$$E(k) = \begin{pmatrix} 0 \\ \beta\epsilon(k) \end{pmatrix}$$

where $\epsilon(k)$ stacks the noise vectors. The disagreement dynamics then become [52]

$$s^d(k+1) = As^d(k) + B_c r^d(k) + B_s P_k r^d(k) + E^d(k)$$

where $E^d(k)$ is the projection of $E(k)$ onto the disagreement subspace [53]. If the noise is bounded or has bounded second moments, and if the homogeneous system is stable and the communication matrices contract disagreement, then the system is input to state stable. This means that the disagreement remains bounded and often converges to a neighborhood of zero whose radius is proportional to the noise magnitude.

The coupling between algorithm parameters and communication imperfections is important. Larger inertia ω and higher gains α and β typically accelerate convergence in ideal conditions but reduce the stability margin and make the system more sensitive to delays and noise. For instance, the stability region in the (ω, κ) plane shrinks when delays are introduced. Similarly, asymmetries in directed graphs can amplify certain disturbances. Nodes with high out degree and low in degree act as leaders whose errors or delays propagate widely, whereas nodes with low outgoing influence have limited impact [54].

From a design perspective, robustness considerations motivate parameter choices that provide sufficient damping of the dynamics. Choosing ω significantly below 1, with moderate values of α and β, tends to yield more overdamped behavior that tolerates delays and noise better, at the cost of slower convergence. The trade offs can be quantified by examining the spectral radius of the linearized system matrix under different parameter combinations and by analyzing worst case contractions of the communication products.

6 Numerical and Design Implications

Although the analysis is conducted in a deterministic mean field setting, it suggests qualitative behaviors that can be observed in numerical experiments and that can guide the design of decentralized particle swarm algorithms. A useful way to interpret the results is to view the swarm

dynamics as a combination of a local second order linear system and an information diffusion process governed by the directed communication graphs.

Consider a numerical scenario in which n particles move in a moderate dimensional space, such as $d = 5$, and the objective function is a smooth, multimodal function with a known global minimum. One can simulate different sequences of directed graphs while keeping the algorithm parameters fixed and compare convergence rates and swarm behavior [55]. For example, using a directed ring as the communication graph at each time step, with edges from particle i to particle $i + 1$ modulo n, yields a topology in which information about good solutions propagates slowly around the ring. In such a case the second largest eigenvalue modulus of the associated row stochastic matrix is close to 1, leading to slow contraction of disagreement.

Numerically, such a ring topology often produces long transients during which different segments of the ring follow different neighborhood bests. Personal bests discovered by one particle take many iterations to influence distant particles. The consensus decomposition explains this behavior: the consensus mode moves according to the local dynamics, but the disagreement modes decay slowly because the communication matrix has weak mixing properties. If the local dynamics are close to marginal stability, the slow decay of disagreement can interact with noise and cause oscillatory or wandering behavior [56].

In contrast, consider a time varying topology in which at each time step a directed random graph is generated with each possible edge present with a certain probability, and directions assigned randomly, but with the constraint that the resulting graph remains weakly connected. Over short time windows, the union of these graphs is likely to be strongly connected and to contain multiple directed spanning trees. The associated products of row stochastic matrices contract disagreement more rapidly, and numerical simulations typically show faster alignment of personal bests and positions. The swarm behavior in such settings resembles that of a centralized algorithm in which a global best is effectively available, because the neighborhood bests across particles become nearly identical.

The graph theoretic analysis suggests that adding even a small fraction of long range edges to a sparse topology can significantly reduce the effective diameter of the communication graph and improve convergence. For instance, augmenting a directed ring with a small number of random directed shortcuts transforms it into a small world network. The eigenvalue spectrum of the associated weight matrices shifts, reducing the magnitude of the second largest eigenvalue and increasing the contraction rate of disagreement [57]. Simulations often confirm that a small number of added edges can lead to substantial convergence acceleration, even when the total communication cost increases only modestly.

The influence structure in directed graphs also affects which particles have dominant impact on the swarm. In graphs with a clear root set that has directed paths to all nodes, personal bests discovered by root particles heavily influence neighborhood bests and hence the motion of the swarm. If root particles explore promising regions, this can lead to faster convergence. However, if root particles become trapped in local minima or are affected by noise or delays, their outsized influence can be detrimental. Graph designs that balance influence by ensuring that root sets change over time or that no small subset of nodes permanently dominates the information flow can improve robustness.

Another practical implication concerns the choice of algorithm parameters in relation to graph properties [58]. When communication is dense and disagreement contracts quickly, one can choose more aggressive parameters, with larger inertia and attraction gains, because the swarm behaves similarly to a centralized system. In contrast, when communication is sparse or intermittent, more conservative parameters may be necessary to ensure stability while disagreement decays. This suggests that parameter tuning should take into account not only the objective function but also communication properties such as graph connectivity, diameter, and variability.

Asynchrony and delays affect design choices as well. In asynchronous implementations where particles update at different rates, the effective contraction per global time unit decreases, and

stability margins shrink. The analysis indicates that reducing inertia and gains can compensate for this reduction and prevent oscillations [59]. When delays in neighborhood best information are significant, using lower inertia and smaller social gains can also help dampen the effect of stale information. Adaptive schemes that adjust parameters based on measured communication quality, such as observed link reliability or update frequency, can be motivated by this viewpoint.

While the linear mean field model abstracts away many nonlinearities and stochastic effects, it captures structural aspects of the interaction between graph topology and swarm dynamics. Numerical studies that implement the full stochastic algorithm with finite populations, random coefficients, and more complex objective functions often exhibit behaviors consistent with the predictions based on the linear model. The decomposition into consensus and disagreement modes provides a lens through which to interpret phase portraits and time series plots of particle positions and velocities. For example, rapid alignment of positions after a transient indicates strong disagreement contraction, whereas persistent clusters moving in different directions suggest slow or incomplete mixing due to graph structure.

In design applications, these insights can be used to synthesize communication protocols and graph structures that satisfy constraints on bandwidth and connectivity while delivering acceptable convergence performance [60]. One can tailor W_k to trade off communication cost and convergence speed by adjusting neighborhood sizes and weights. For instance, giving slightly higher weight to neighbors that are information hubs can speed up consensus but may increase vulnerability to failures at those nodes. Conversely, more uniform weighting can distribute influence more evenly and enhance robustness at the expense of slower convergence.

7 Conclusion

Decentralized particle swarm optimization over directed, time varying communication graphs exhibits a rich interplay between local particle dynamics and global information diffusion. By modeling the mean dynamics using linear systems and encoding the communication structure through products of row stochastic matrices, one can obtain convergence guarantees that separate the influence of algorithm parameters from that of graph topology. The decomposition of the swarm state into consensus and disagreement components reveals that the consensus dynamics reduce to those of a single particle driven by averaged best information, while the disagreement dynamics are governed by the connectivity and temporal patterns of the directed graphs.

Under assumptions that the objective function has a strict local minimum, that the gains defining the particle updates yield a stable linearization around this minimum, and that the sequence of communication graphs is jointly rooted with uniformly positive weights, the analysis shows that disagreement in personal bests and in particle states decays to zero [61]. All particles then converge to a common position and velocity, and their personal bests agree. The directed, time varying graphs affect the speed and intermediate patterns of this convergence but do not prevent agreement as long as persistent connectivity conditions hold.

Extensions of the framework to account for asynchronous updates, bounded communication delays, random link failures, and measurement noise illustrate that similar qualitative conclusions can be reached in more realistic settings, provided that the effective communication matrices retain contraction properties and that disturbances remain bounded. In such cases the swarm converges to a neighborhood of the equilibrium, with the size of this neighborhood determined by the disturbance characteristics and the stability margins of the linearized dynamics.

The graph theoretic perspective developed here provides structural insight into how directed, time varying communication patterns shape the behavior of decentralized particle swarms. It suggests that convergence performance can be improved by designing communication graphs that are jointly well connected, by tuning particle update gains in accordance with graph properties, and by managing the trade offs between convergence speed and robustness to imperfections. While the analysis focuses on mean field and local properties, the conceptual separation between consensus and disagreement modes offers a foundation for further studies that incorpo-

rate more detailed models of stochastic effects, nonlinearities, and complex objective landscapes in decentralized swarm optimization [62].

References

[1] D. K. N. Dechmann, S. L. Heucke, L. Giuggioli, K. Safi, C. C. Voigt, and M. Wikelski, "Experimental evidence for group hunting via eavesdropping in echolocating bats," *Proceedings. Biological sciences*, vol. 276, pp. 2721–2728, 5 2009.

[2] A. Fernandes, M. S. Couceiro, D. Portugal, J. M. Santos, and R. P. Rocha, "Ad hoc communication in teams of mobile robots using zigbee technology," *Computer Applications in Engineering Education*, vol. 23, pp. 733–745, 4 2015.

[3] C. Samuelsson, "Fedcsis (communication papers) - the revised stochastic simplex bisection algorithm and particle swarm optimization.," in *Annals of Computer Science and Information Systems*, vol. 13, pp. 103–110, IEEE, 9 2017.

[4] C. Ramachandran, R. Malik, X. Jin, J. Gao, K. Nahrstedt, and J. Han, "Videomule: a consensus learning approach to multi-label classification from noisy user-generated videos," in *Proceedings of the 17th ACM international conference on Multimedia*, pp. 721–724, 2009.

[5] N. Nashikkar, D. Begde, S. Bundale, M. Pise, J. Rudra, A. Upadhyay, and A. Upadhya, 3 2011.

[6] S. Devi, A. K. Jagadev, and S. Dehuri, *Multi-objective Swarm Intelligence - Comparison of Various Approaches in Multi-objective Particle Swarm Optimization (MOPSO): Empirical Study*. Germany: Springer Berlin Heidelberg, 3 2015.

[7] S. Hoshino, R. Takisawa, and Y. Kodama, "Swarm robotic systems based on collective behavior of chloroplasts," *Journal of Robotics and Mechatronics*, vol. 29, pp. 602–612, 6 2017.

[8] P. Umarani and P. Thangaraj, "Improving group communication in wireless telemedicine system using fish swarm algorithm," *Journal of Medical Imaging and Health Informatics*, vol. 6, pp. 1576–1580, 11 2016.

[9] H. M. H. N. Bandara, O. Lam, L. Jin, and L. P. Samaranayake, "Microbial chemical signaling: a current perspective.," *Critical reviews in microbiology*, vol. 38, pp. 217–249, 2 2012.

[10] V. Loscri, E. Natalizio, V. Mannara, and G. Aloi, *BIONETICS - A Novel Communication Technique for Nanobots Based on Acoustic Signals*, pp. 91–104. Germany: Springer International Publishing, 7 2014.

[11] R. Islam, I. Mobin, M. N. Shakib, and M. M. Rahman, "An approach of ir-based short-range correspondence systems for swarm robot balanced requisitions and communications," 1 2016.

[12] K. Sugawara and Y. Doi, *ICIRA (1) - Collective Construction by Cooperation of Simple Robots and Intelligent Blocks*, pp. 452–461. Germany: Springer International Publishing, 8 2016.

[13] R. Chandrasekar, V. Vijaykumar, and T. Srinivasan, "Probabilistic ant based clustering for distributed databases," in *2006 3rd International IEEE Conference Intelligent Systems*, pp. 538–545, IEEE, 2006.

[14] M. Thangaraj and P. P. Ponmalar, *KMO - Swarm Intelligence Based Data Aggregation for Intruder Detection in Wireless Sensor Networks*. Germany: Springer International Publishing, 8 2015.

[15] M. Krishnaveni, P. Subashini, and T. T. Dhivyaprabha, "Improved canny edges using cellular based particle swarm optimization technique for tamil sign digital images," *International Journal of Electrical and Computer Engineering (IJECE)*, vol. 6, pp. 2158–2166, 10 2016.

[16] F. Saffre and A. Simaitis, "Host selection through collective decision," *ACM Transactions on Autonomous and Adaptive Systems*, vol. 7, pp. 4–16, 5 2012.

[17] "Practical swarm optimization based fault-tolerance algorithm for the internet of things," *KSII Transactions on Internet and Information Systems*, vol. 8, pp. 1178–1191, 4 2014.

[18] D. Ruby, M. Vijayalakshmi, and A. Kannan, "Intelligent relay selection and spectrum sharing techniques for cognitive radio networks," *Cluster Computing*, vol. 22, pp. 10537–10548, 8 2017.

[19] E. Tuci, B. Mitavskiy, and G. Francesca, "Ecal - on the evolution of self-organised role-allocation and role-switching behaviour in swarm robotics: a case study," in *Advances in Artificial Life, ECAL 2013*, vol. 12, pp. 379–386, MIT Press, 9 2013.

[20] M. Hartbauer and H. Römer, "A novel distributed swarm control strategy based on coupled signal oscillators," *Bioinspiration & biomimetics*, vol. 2, pp. 42–56, 9 2007.

[21] S. R. Shinge and S. S. Sambare, "Survey of different clustering algorithms used to increase the lifetime of wireless sensor networks," *International Journal of Computer Applications*, vol. 108, pp. 15–18, 12 2014.

[22] T. Srinivasan, V. Vijaykumar, and R. Chandrasekar, "An auction based task allocation scheme for power-aware intrusion detection in wireless ad-hoc networks," in *2006 IFIP International Conference on Wireless and Optical Communications Networks*, pp. 5–pp, IEEE, 2006.

[23] S. K. Rakesh, B. Choudhary, and R. Sandhu, "Cooperative problem solving in telecommunication network," *INTERNATIONAL JOURNAL OF MANAGEMENT & INFORMATION TECHNOLOGY*, vol. 4, pp. 388–392, 7 2013.

[24] R. Bouffanais, *Outlook: Can Swarms Be Designed?*, pp. 105–106. Springer Singapore, 10 2015.

[25] Z. Afzal, P. A. Shah, K. M. Awan, and null Zahoor-ur Rehman, "Optimum bandwidth allocation in wireless networks using differential evolution," *Journal of Ambient Intelligence and Humanized Computing*, vol. 10, pp. 1401–1412, 5 2018.

[26] S. Sharma, A. K. Giri, and N. Singhal, "Finding optimal configuration of dsdv using particle swarm optimization," *International Journal of Computer Applications*, vol. 104, pp. 27–31, 10 2014.

[27] U. R. Zimmer and N. Kottege, "Acoustical methods for azimuth, range and heading estimation in underwater swarms," *The Journal of the Acoustical Society of America*, vol. 123, pp. 3007–3007, 5 2008.

[28] V. P. Singh, P. Samuel, and N. Kishor, "Impact of demand response for frequency regulation in two-area thermal power system," *International Transactions on Electrical Energy Systems*, vol. 27, pp. e2246–, 8 2016.

[29] C. Gershenson, "Complexity at large," *Complexity*, vol. 16, pp. 1–4, 9 2010.

[30] B. Li, "Particle swarm optimization for radar binary phase code selection," in *Radar Sensor Technology XXII*, vol. 10633, pp. 9–, SPIE, 5 2018.

[31] C. Ramachandran, S. Misra, and M. Obaidat, "On evaluating some agent-based intrusion detection schemes in mobile ad-hoc networks," in *Proceedings of the SPECTS 2007*, (San Diego, CA), pp. 594–601, July 2007.

[32] A. Kroeller, S. P. Fekete, D. Pfisterer, and S. Fischer, "Deterministic boundary recognition and topology extraction for large sensor networks," 1 2005.

[33] J. A. Carrillo, Y.-P. Choi, M. Hauray, and S. Salem, "Mean-field limit for collective behavior models with sharp sensitivity regions," *Journal of the European Mathematical Society*, vol. 21, pp. 121–161, 9 2018.

[34] N. Kimura, "Metagenomic approaches to understanding phylogenetic diversity in quorum sensing," *Virulence*, vol. 5, pp. 433–442, 2 2014.

[35] J. Yu, B. Wang, X. Du, Q. Wang, and L. Zhang, "Ultra-extensible ribbon-like magnetic microswarm.," *Nature communications*, vol. 9, pp. 3260–, 8 2018.

[36] M. R. Khan, A. Sadeed, A. Asad, Z. Tariq, and M. Tauqeer, "Maximizing oil recovery in a naturally fractured carbonate reservoir using computational intelligence based on particle swarm optimization," in *PAPG/SPE Pakistan Section Annual Technical Conference and Exhibition*, SPE, 12 2018.

[37] P. M. Putora and J. Oldenburg, "Swarm-based medicine," *Journal of medical Internet research*, vol. 15, pp. e207–, 9 2013.

[38] M. Ismail, N. Javaid, M. Zakria, M. Zubair, F. Saeed, and M. A. Zaheer, *NBiS - Cloud-Fog Based Smart Grid Paradigm for Effective Resource Distribution*, pp. 234–247. Springer International Publishing, 8 2018.

[39] L. Sun, L. Wang, and H. Ge, "A coevolutionary bacterial foraging model using pso in job-shop scheduling environments," *International Journal of Grid and Distributed Computing*, vol. 9, pp. 379–394, 9 2016.

[40] V. Vijaykumar, R. Chandrasekar, and T. Srinivasan, "An ant odor analysis approach to the ant colony optimization algorithm for data-aggregation in wireless sensor networks," in *2006 International Conference on Wireless Communications, Networking and Mobile Computing*, pp. 1–4, IEEE, 2006.

[41] V. Jha, S. Deol, M. Jha, and G. K. Sharma, "Energy and latency aware application mapping algorithm & optimization for homogeneous 3d network on chip," in *Computer Science & Information Technology (CS & IT)*, pp. 13–27, Academy & Industry Research Collaboration Center (AIRCC), 3 2014.

[42] M. Manjunath and D. H. Manjaiah, $SS_PAR : SignalStrengthBasedPetalAntRoutingAlgorithmforMo$ $-217. SpringerIndia, 82015.$

[43] I. Computing, S.-I. Ao, O. Castillo, and X. Huang, *Intelligent Control and Innovative Computing - Intelligent control and innovative computing*. Germany: Springer New York, 12 2011.

[44] A. Garcia, "Bio-inspired schemes for global optimization and online distributed search," 4 2012.

[45] H. S. Kotian, S. Harkar, S. Joge, A. K. Mishra, A. Zafal, V. Singh, and M. M. Varma, "Spatial awareness of a bacterial swarm," 6 2018.

[46] S. Q. Ameen and F. L. Khaleel, "Wireless mesh networks based on mbpso algorithm to improvement throughput," *International Journal of Electrical and Computer Engineering (IJECE)*, vol. 8, pp. 4374–4381, 12 2018.

[47] O. Ben-Shahar, S. Dolev, A. Dolgin, and M. Segal, "Dialm-podc - direction election in flocking swarms," in *Proceedings of the 6th International Workshop on Foundations of Mobile Computing*, pp. 73–80, ACM, 9 2010.

[48] I. Sokolov, V. R. Cherkasov, A. Tregubov, S. R. Buiucli, and M. P. Nikitin, "Smart materials on the way to theranostic nanorobots: Molecular machines and nanomotors, advanced biosensors, and intelligent vehicles for drug delivery.," *Biochimica et biophysica acta. General subjects*, vol. 1861, pp. 1530–1544, 1 2017.

[49] T. Srinivasan, R. Chandrasekar, V. Vijaykumar, V. Mahadevan, A. Meyyappan, and M. Nivedita, "Exploring the synergism of a multiple auction-based task allocation scheme for power-aware intrusion detection in wireless ad-hoc networks," in *2006 10th IEEE Singapore International Conference on Communication Systems*, pp. 1–5, IEEE, 2006.

[50] S. Hanna, H. Yan, and D. Cabric, "Distributed uav placement optimization for cooperative line-of-sight mimo communications," 1 2018.

[51] Y. Li, J. Klingner, and N. Correll, "Distributed camouflage for swarm robotics and smart materials," *Autonomous Robots*, vol. 42, pp. 1635–1650, 2 2018.

[52] R.-M. Chen and D.-S. Wu, "Solving scheduling problem using particle swarm optimization with novel curve based inertia weight and grouped communication topology," *International Journal of Digital Content Technology and its Applications*, vol. 7, pp. 94–103, 4 2013.

[53] S. Renier, M. Hébraud, and M. Desvaux, "Molecular biology of surface colonization by listeria monocytogenes: an additional facet of an opportunistic gram-positive foodborne pathogen," *Environmental microbiology*, vol. 13, pp. 835–850, 11 2010.

[54] K.-C. Lin, W.-C. Li, and J. C. Hung, *Detection for Different Type Botnets Using Feature Subset Selection*, pp. 523–529. Germany: Springer Singapore, 4 2016.

[55] R. N. Akram, K. Markantonakis, K. Mayes, O. Habachi, D. Sauveron, A. Steyven, and S. Chaumette, "Security, privacy and safety evaluation of dynamic and static fleets of drones," 1 2017.

[56] P. Martínez, P. Huedo, S. Martínez-Servat, R. Planell, M. Ferrer-Navarro, X. Daura, D. Yero, and I. Gibert, "Stenotrophomonas maltophilia responds to exogenous ahl signals through the luxr solo smor (smlt1839)," *Frontiers in cellular and infection microbiology*, vol. 5, pp. 41–41, 5 2015.

[57] F. Al-Turjman and S. Alturjman, "5g/iot-enabled uavs for multimedia delivery in industry-oriented applications," *Multimedia Tools and Applications*, vol. 79, pp. 8627–8648, 6 2018.

[58] C. Yinka-Banjo, I. O. Osunmakinde, and A. Bagula, "Cooperative behaviours with swarm intelligence in multirobot systems for safety inspections in underground terrains," *Mathematical Problems in Engineering*, vol. 2014, pp. 1–20, 7 2014.

[59] R. Chandrasekar and S. Misra, "Using zonal agent distribution effectively for routing in mobile ad hoc networks," *International Journal of Ad Hoc and Ubiquitous Computing*, vol. 3, no. 2, pp. 82–89, 2008.

[60] M. F. Rohman, F. Rofii, and F. Hunaini, "Optimasi penempatan menara bts menggunakan quantum-behaved particle swarm optimization," *JURNAL NASIONAL TEKNIK ELEKTRO*, vol. 5, pp. 308–314, 10 2016.

[61] K. Lenin, "Green darner algorithm for solving optimal power flow problem," *International Journal of Research -GRANTHAALAYAH*, vol. 5, pp. 106–115, 9 2017.

[62] A. Hashim, T. Saini, H. Bhardwaj, A. Jothi, and A. V. Kumar, *Application of Swarm Intelligence in Autonomous Cars for Obstacle Avoidance*, pp. 393–404. Germany: Springer Singapore, 9 2018.